Transactions of the Karelian Research Centre of the
Russian Academy of Sciences
No. 9. 2019. P. 125–135
DOI: 10.17076/lim1107

Труды Карельского научного центра РАН
№ 9. 2019. С. 125–135

УДК 551.46.06 + 528.8.04

SATELLITE EVIDENCE FOR ENHANCEMENT OF THE COLUMN MIXING RATIO OF ATMOSPHERIC CO_2 OVER *E. HUXLEYI* BLOOMS

D. V. Kondrik[1], E. E. Kazakov[1], D. V. Pozdnyakov[1], O. M. Johannessen[2]

[1] Nansen International Environmental and Remote Sensing Centre, St. Petersburg, Russia
[2] Nansen Scientific Society, Bergen, Norway

Emiliania huxleyi algae are known to enhance CO_2 partial pressure in their ambient water, $(pCO_2)_w$. Thus, over such bloom areas, the atmospheric column-averaged dry air mole fraction of carbon dioxide (XCO_2) is likely to increase, which has not yet been quantified on basin scales. Here we report on an Orbiting Carbon Observatory (OCO-2) satellite study of the influence of *E. huxleyi* blooms on XCO_2 over the Black Sea. We established that concurrently with a significant $(pCO_2)_w$ rise, there was an increase in the overlying XCO_2 within the range ~1 to nearly 2 ppmv, which is commensurate with the planetary annual increase of XCO_2. As we found, $(\Delta pCO_2)_w$ in the Black Sea and Subpolar and Polar seas are closely comparable. This strongly indicates that *E. huxleyi* blooms do weaken carbon sinks in the ocean on a large scale, which can be consequential for global climatology and marine biogeochemistry.

Keywords: Black Sea; blooms of *Emiliania huxleyi*; CO_2 partial pressure in water; satellite remote sensing; OCO-2 data; enhancement of atmospheric columnar CO_2 content over *E. huxleyi* blooms.

Д. В. Кондрик, Э. Э. Казаков, Д. В. Поздняков, О. М. Йоханнессен. СПУТНИКОВОЕ ДОКАЗАТЕЛЬСТВО УВЕЛИЧЕНИЯ КОНЦЕНТРАЦИИ CO_2 В АТМОСФЕРНОМ СТОЛБЕ НАД ОБЛАСТЬЮ ЦВЕТЕНИЯ *E. HUXLEYI*

Известно, что водоросли *Emiliania huxleyi* повышают парциальное давление CO_2 в окружающей их воде, $(pCO_2)_w$. Таким образом, над областями цветения может увеличиваться средняя по атмосферному столбу мольная доля диоксида углерода (XCO_2) сухого воздуха. Значения (XCO_2) количественно еще не определялись в масштабах бассейна. Здесь мы сообщаем о спутниковом исследовании влияния цветений *E. huxleyi* на значения XCO_2 над Черным морем, основанном на данных Orbiting Carbon Observatory (OCO-2). Установлено, что одновременно со значительным увеличением $(pCO_2)_w$ в атмосферном столбе над цветением наблюдается увеличение XCO_2 в диапазоне от ~ 1 до почти 2 ppmv, что по величине сравнимо с планетарным годовым увеличением XCO_2. Показано, что значения $(pCO_2)_w$ в Черном море и в субполярных и полярных морях тесно сопоставимы. Это убедительно свидетельствует о том, что цветения *E. huxleyi* в значительной степени ослабляют способность океана поглощать углерод на значительных протяженностях, и это может иметь значение для глобальной климатологии и морской биогеохимии.

Ключевые слова: Черное море; цветения *Emiliania huxleyi*; парциальное давление CO_2 в воде; спутниковое дистанционное зондирование; данные OCO-2; возрастание содержания CO_2 в атмосферном столбе над цветениями *Emiliania huxleyi*.

Introduction

Phytoplankton blooms of *Emiliania huxleyi* are known to produce CO_2, causing less uptake of atmospheric CO_2 by the ocean. A recent study based on 18 years (1998–2015) of quantitative satellite observations of CO_2 partial pressure in surface waters, $(pCO_2)_w$ of five seas in the North Atlantic, Arctic and North Pacific, revealed that within the areas of *E. huxleyi* blooms, the increment in pCO_2, $(\Delta pCO_2)_w$ was significant, constituting tens to hundreds of microatmospheres [Kondrik et al., 2018; the respective database and its description can be found in Kondrik et al., 2019].

When normalized to CO_2 partial pressure in the absence of blooms ("background" pCO_2 in water – $(pCO_2)_{wb}$), the mean and maximum $(\Delta pCO_2)_w$ values proved to be in the range 20.4–44.2 and 31.6–62.5 %, respectively. The bloom areas in the target seas varied significantly among the years with maximum values in the range of several tens to several hundreds of square kilometres [Kondrik et al., 2017].

The aforementioned *E. huxleyi* bloom-driven enhancement of dissolved CO_2 partial pressure can reduce, nullify or even reverse the flux of CO_2 at the atmosphere-ocean interface. Indeed, Shutler et al. [2013] report on an average reduction in the monthly air-sea CO_2 flux by about 55 % across the marine tracts encompassing extensive *E. huxleyi* blooms in the North Atlantic, whereas the maximum reduction over the time period 1998–2007 was registered at 155 %.

In the southern hemisphere *E. huxleyi* blooms are also vast: e. g., the area of the gigantic Great Calcite Belt extending from ~ 38 to ~ 60 °S is reportedly in excess of 50 million square kilometres [Balch et al., 2016].

Given these estimations, it is reasonable to expect that at least within the areas of *E. huxleyi* blooms, the CO_2 balance between the atmosphere and the ocean can shift, causing a considerable reduction in the CO_2 flux from atmosphere to ocean and even its reversal.

Due to the global nature of the phenomenon of *E. huxleyi* blooms [Brown, Yoder, 1994; Iglesias-Rodrigues et al., 2002; Moore et al., 2012], this can have appreciable ramifications, among which are a reduction in the world's ocean carbon sink and a consequential enhancement of global warming [IPCC, 2014].

However, until recently, numerical assessments of the impact of *E. huxleyi* blooms on CO_2 exchange between atmosphere and ocean were confined to isolated shipborne *in situ* measurements [e. g. Robertson et al., 1994], and as such could not be considered representative because of data paucity. With the launch of the Orbiting Carbon Observatory 2 (OCO-2) satellite mission [Crisp, 2015] in 2014 such studies became feasible: the column-averaged dry air mole fraction of carbon dioxide (XCO_2) retrieved by OCO-2 can be obtained over the target bloom of *E. huxleyi* in order to detect the XCO_2 enhancement in the atmosphere.

Here we report on the results of our satellite study of the Black Sea, as a test example. The reason for this selection is twofold: firstly, the Black Sea is an area of intense *E. huxleyi* blooms [Cokacar et al., 2001], and secondly, such intense blooms occur there annually, in contrast to other seas [Smyth et al., 2004; Oguz, Merico, 2006]. At the maximum of their development (e. g. in 2012), the blooms cover areas as large as ~ 354×10^3 km^2, thus accounting for ~ 84 % of the entire surface of the sea.

Materials and Methods

To implement the present study, spatially and temporally collocated data on two remotely-sensed variables are required, viz. on spectral remote sensing reflectance, R_{rs}(sr^{-1}) and XCO_2 (ppmv). These data are from, respectively, OC CCI (in six channels centred at 412, 443, 490, 510, 555 and 670 nm, at 4 km spatial and 8 day temporal resolution, http://www.esa-oceancolour-cci.org) and OCO-2 (OCO-2 Level 2 bias-corrected XCO_2 product at 3 km^2 spatial resolution, NASA Data Archive Page https://disc.gsfc.nasa.gov/datasets?project=OCO).

The period of satellite observations covers two years (2015–2016), when both Ocean Colour Climate Change Initiative (OC CCI) and OCO-2 data were available. Although also available for 2017 and 2018, OCO-2 data could not be used as they proved to be deficient due to either extensive cloud masking or heavy flagging (the prevailing amount of data points contained low-quality flags) over the areas encompassing OCO-2 footprint trajectories within *E. huxleyi* blooms in the Black Sea.

The work was performed in the following major sequential steps: (1) identification and precise delineation/quantification of an *E. huxleyi* bloom area, (2) quantification of the enhancement of CO_2 partial pressure in surface water, $(\Delta pCO_2)_w$ (μatm) within the bloom area, (3) identification of XCO_2 (ppmv) data availability on the target marine areas, (4) establishment of XCO_2 variations over the target area, and (5) quantification of increments in XCO_2, ΔXCO_2 during the bloom period against the respective XCO_2 background values.

The methodologies of fulfilling steps 1 and 2 are described in detail in our previous papers [Kondrik et al., 2017, 2018]. Here only their brief descriptions are given.

In step 1, spectra of R_{rs} from the turquoise areas produced by *E. huxleyi* algae were automatically analyzed to select those complying with the preselected thresholds and the location of maxima for this variable at the OC CCI wavelengths in the visible. Summation of the pixels thus identified gave the bloom area.

In step 2, values of CO_2 partial pressure in surface waters, $(\Delta pCO_2)_w$ within the bloom area were obtained making use of the algorithm developed in [Kondrik et al., 2018]. The algorithm is based on the regression dependency between the values of R_{rs} (490 nm) and $(\Delta pCO_2)_w$, which has been confidently established with the root mean square error of +/–23.4 µatm on the basis of more than 2500 data points located throughout the subarctic and arctic seas.

In step 3, XCO_2 data from OCO-2 were selected that conformed to a single-sounding random error between 0.5 and 1 ppmv [Crisp, 2015] and respective quality control flags.

Step 4. Some XCO_2 values were not available for each 8-day intervals of observations because of either cloud filtering or OCO-2 data flagging/ unreliable quality. To fill such gaps in the sequence of XCO_2 values, i. e. the missing segments of the XCO_2 intraannual variations, a linear interpolation approach was employed. Further, the sequence of XCO_2 values was subjected to a polynomial approximation of order 7.

This approach was applied separately to both (*i*) all data over the entire two-year term (i. e. 2015–2016), including the periods of *E. huxleyi* blooming, and (*ii*) to the data registered each year but excluding the *E. huxleyi* blooming period per se plus one week before and after the blooming.

The difference ΔXCO_2 between the *actually recorded XCO_2 values* and the respective *approximated XCO_2 values beyond the E. huxleyi blooming period* reflects for the excess of XCO_2 over the bloom area.

In step 5, ΔXCO_2 values were quantified and their temporal variability was analyzed.

Results

Our quantitative assessments of the *E. huxleyi* bloom extent in the target sea indicate that we are dealing with a huge phenomenon. Indeed, as Figure 1, *a* illustrates, both in 2015 and 2016 the bloom areas at the stage of maximum development reached 177.0–205.3 thousand square kilometers, which corresponds to 41.9–48.6 %, i. e. almost half of the entire surface of the Black Sea with depths in excess of 200 m (e. g. [Özsoy, Ünlüata, 1997], see also Figure 2, *a*).

Importantly, for the periods of blooming in 2015 and 2016, the concurrent OCO-2 daily data are in most cases amply available with only rare exceptions (black bars in Figure 1, *a*).

The obtained data reveal enhanced values of XCO_2 over the bloom areas. The magnitude of XCO_2 increment for both years proved to be significant: the maximum increments of XCO_2 are close to 2 ppmv (Fig. 1, *c*), which constitutes ~ 0.5 % of the present mean pCO_2 in the atmosphere [Dlugokencky, 2016] or is on the same order of magnitude as the annual increase. Given that (*i*) the single-sounding random errors are between 0.5 and 1 ppmv [Crisp, 2015] and (*ii*) the number of OCO-2 observations in our case is up to 400 (Fig. 1, *a*), the increments established in this study should generally be considered as reliable. An independent confirmation of validity of this statement can be found e. g. in [Wu et al., 2018].

However, there was one case on 24.05.2016 when the XCO_2 increment value was highly negative, about ~1.5 ppmv, i. e. beyond the stated error of a single sounding, 0.5–1.0 ppmv. This case corresponds to the situation when the number of return signals was at least ten times less than that registered in other measurements during the period of high bloom intensity (compare Fig. 1, *a* and *c*), and hence the respective retrievals were insufficiently reliable. This case is illustrated in Figure 2, *a*: for 24.05.2016 the number of red points (reflecting the OCO-2 footprints) in the marginal eastern part of the sea is far less than for e. g., 16.05.2016 (Fig. 2, *b*) – the date of concurrently high values of max $(\Delta pCO_2)_w$ in surface water and the number of satellite observations and strongly positive XCO_2 increment. The same arguments refer to a few cases in 2015 (Fig. 1, *c*), when the resultant ΔXCO_2 values, although very small, were non-positive.

As the Black Sea is essentially a landlocked waterbody, the influence of watershed-based CO_2 sources (both of rural and industrial/urban origin) can affect XCO_2 readings through the transport of polluted atmospheric air over the *E. huxleyi* blooms. A good clarification of this issue could be the situation when satellite footprints passed through both the bloom and bloom-free areas during one and same overflight. Because of the paucity of high quality OCO-2 data during 2015–2016 on the Black Sea (no clouds, no heavy data flagging) such situations were found solely on two occasions, viz. on 02.06.2015 and 16.05.2016 (Fig. 3 and 2, *b*, respectively). The mean XCO_2 values (in ppmv) over the long footprint passing through the area of *E. huxleyi* bloom, and two footprint segments intersecting the bloom-free area (both are encircled in Fig. 3)

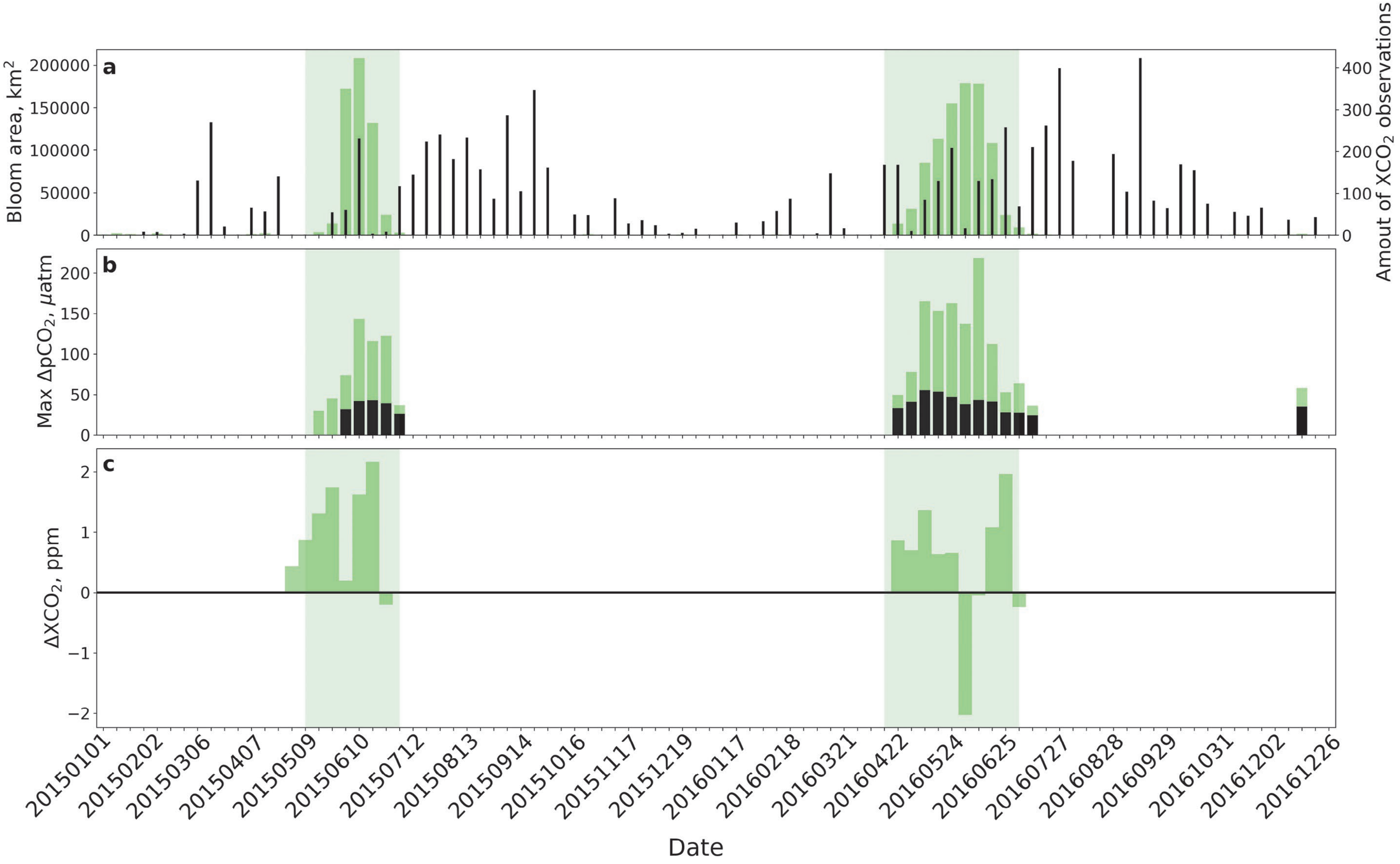

Fig. 1. The phenomenon and effects of *E. huxleyi* blooms in the Black Sea in 2015 and 2016 as observed and characterized from satellite sensors. Panel *a*: (*i*) bloom area (green bars), and (*ii*) number of XCO_2 observations (black bars); panel *b*: $(\Delta pCO_2)_w$ maximal values in water within the bloom area (green bars); panel *c*: XCO_2 increments over the bloom areas. The pale green columns in panels *a*-*c* reflect the period of blooming

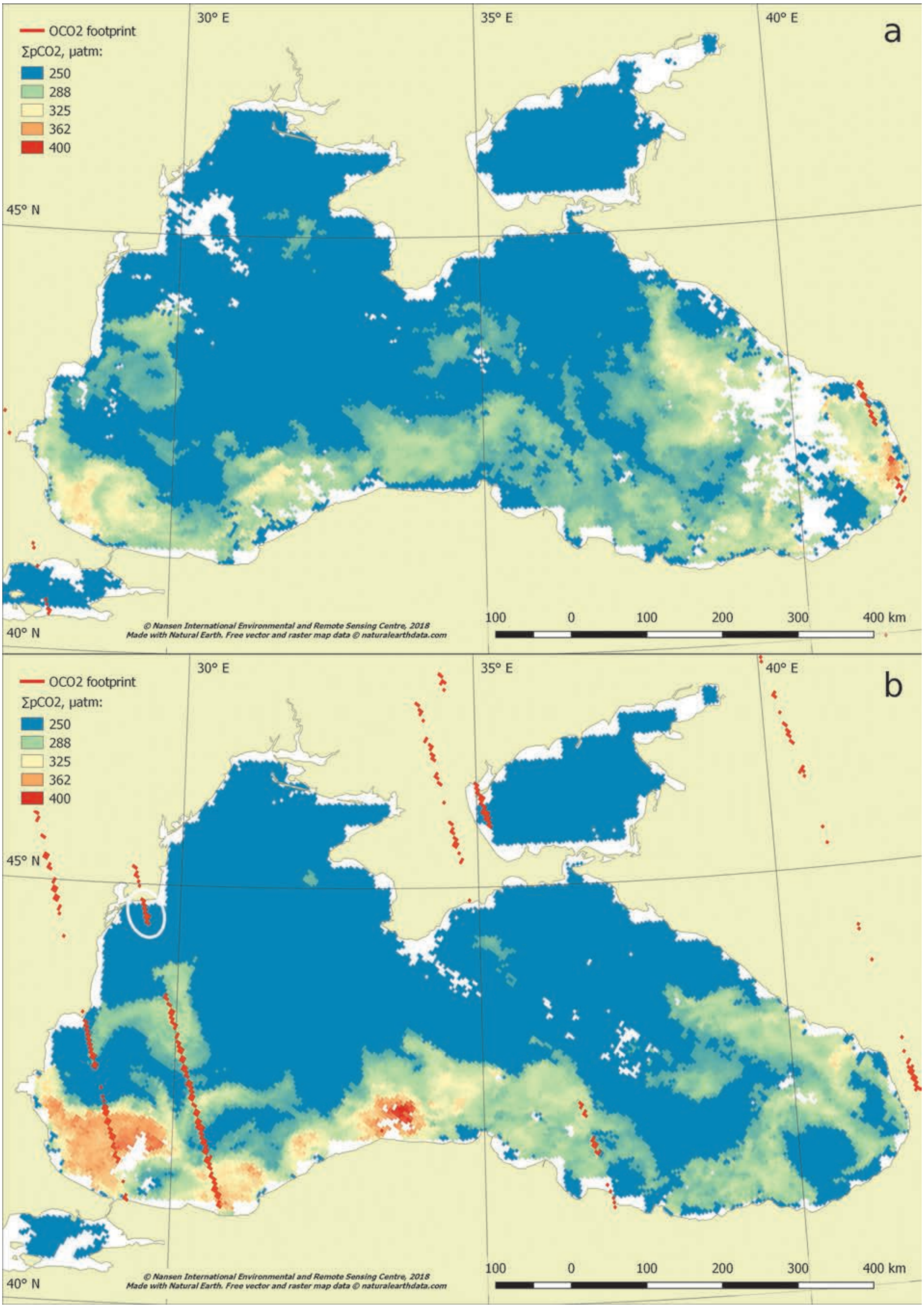

Fig. 2. Spatial distribution of CO$_2$ partial pressure increment, $(\Delta p\mathrm{CO}_2)_w$, in the Black Sea surface water as retrieved from OC CCI data on a) 24.05.2016 and b) 16.05.2016. Red lines are the locations of the OCO-2 footprints across the *E. huxleyi* bloom on each of the two dates. The encircled area is explained in the text

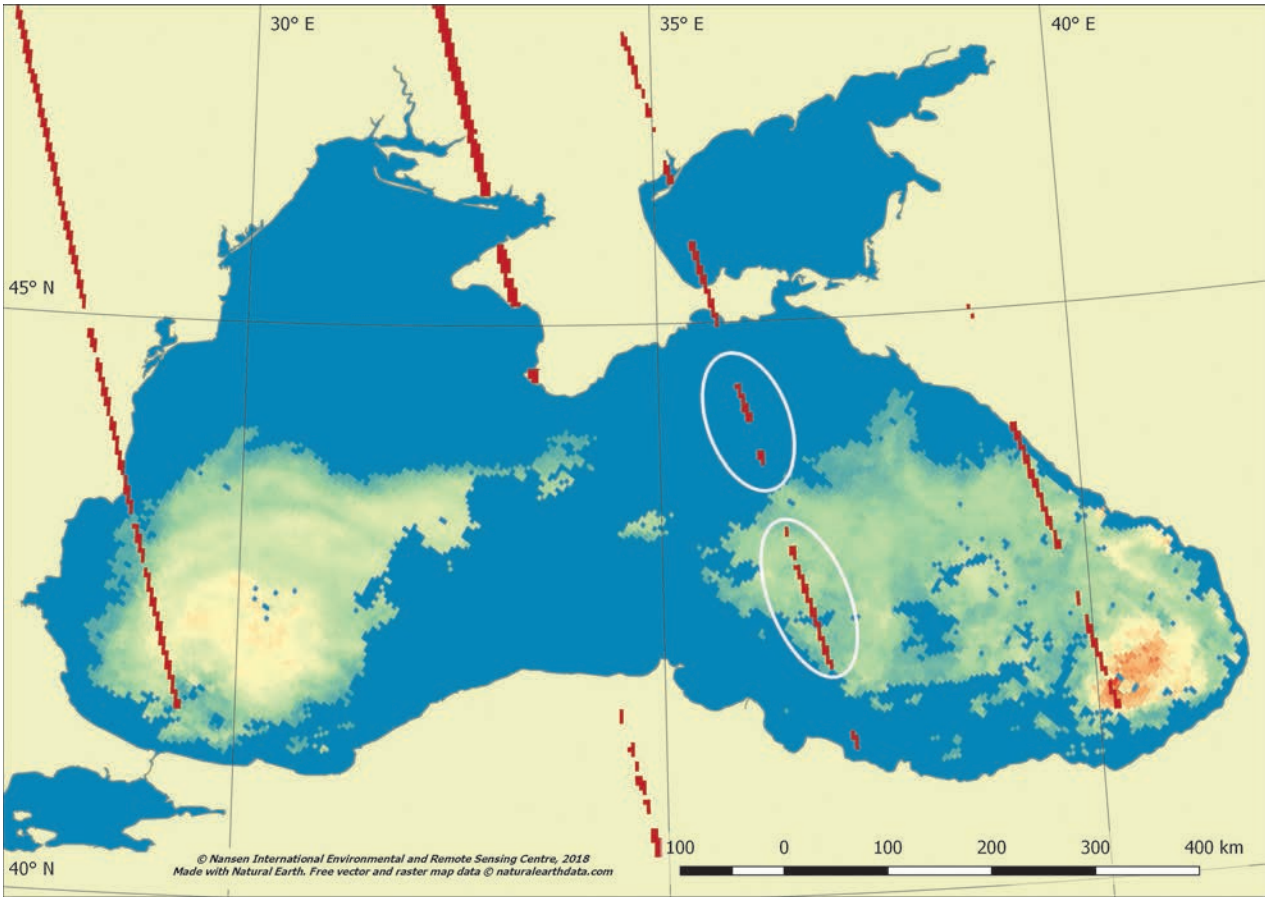

Fig. 3. Spatial distribution of CO_2 partial pressure increment, $(\Delta pCO_2)_w$, in the Black Sea surface water as retrieved from OC CCI data on 02.06.2015.

Red lines designate the OCO-2 footprints across the sea. The encircled areas are explained in the text

were, respectively, 400.07 and 399.2. Thus, these data indicate that there was no significant influence exerted by CO_2 atmospheric advection from the watershed. The same conclusion can be drawn from the second example: on 16.05.2065 the mean XCO_2 values (in ppmv) along the footprint extending over the south-western region of the Black Sea, and along a short part of it (encircled in Fig. 2, *b*) in the close vicinity of the coast were, respectively, 403.5 and 401.75. Should there be any CO_2 atmospheric advection from the watershed, the proportion between these two numbers would be essentially different. Both results should not be considered as incidental. Indeed, all available XCO_2 data registered along the footprints (which passed through different parts of the sea) were used collectively, and on this basis common statistical characteristics were calculated. In other words, there was no specific reference to a concrete point in the footprint, but a general aggregation of spatio-temporal variability in XCO_2 was established. Had there been an impact of CO_2 advection, it would have been reflected in the entire set of XCO_2 determined along the footprint.

Finally, as mentioned above, on some occasions in 2015 and 2016 ΔXCO_2 values are negative (Fig. 1, plate *c*). Although we assume that the negative ΔXCO_2 values are not reliable because they were retrieved from a small number of OCO-2 return signals, nevertheless, they can arguably be interpreted as an explicit indication of the absence of advected CO_2 from the marine watershed in those parts of the sea.

Excluding the unreliable data discussed immediately above leads to a value of the mean XCO_2 increment over the blooming period close to 1 ppmv. Given that this assessment is based on a statistically significant number of measurements (Fig. 1, *a*), it should be assumed as reliable, and hence the trustworthy range of XCO_2 increments over the Black Sea extends from 1 ppmv to the maximum observed value close to 2 ppmv (Fig. 1, *c*).

As our ΔpCO_2 retrieval algorithm was developed and verified for high latitude marine environments, the appropriateness of its application to the conditions of the Black Sea needed confirmation. To the best of our knowledge, there are no

Temporal pattern of CO_2 partial pressure excess (in percent) within *E. huxleyi* blooms in surface waters of the target seas over the period of spaceborne observations (1998–2016)

Year	A					
	North Sea (750)*	Norwegian Sea (1383)	Greenland Sea (1205)	Barents Sea (1400)	Bering Sea (2292)	Black Sea (436)
1998	31.8 (9.6 ; 0.4)**	35.6 (67.0; 12.2)	– (2.8; 0.2)	40.6 (118.4; 8.1)	62.3 (220.2; 8.9)	21.7 (74.2; 17.6)
1999	43.1 (28.1; 1.2)	28.8 (65.1; 11.9)	20.0 (17.2; 1.4)	42.5 (186.1; 12.8)	54.3 (201.2; 8.1)	25.8 (13.8; 3.3)
2000	35.4 (58.9; 2.5)	24.6 (59.6; 10.9)	– (1.2; 0.1)	34.5 (178.0; 12.2)	53.7 (247.3; 10.0)	35.8 (104.9; 24.8)
2001	27.7 (43.9; 1.9)	26.3 (36.7; 6.7)	21.1 (5.8; 0.5)	62.5 (269.4; 18.5)	19.2 (209.0; 8.4)	12.8 (1.7; 0.4)
2002	23.9 (76.4; 3.2)	15.6 (36.4; 6.7)	31.0 (5.2; 0.4)	39.2 (248.0; 17.0)	17.0 (5.5; 0.2)	36.7 (345.2; 81.8)
2003	38.1 (72.6; 3.1)	39.1 (105.4; 19.3)	– (4.8; 0.4)	50.6 (201.9; 13.8)	22.0 (27.0; 1.1)	11.8 (20.1; 4.8)
2004	27.9 (24.8; 1.0)	20.8 (30.7; 5.6)	12.5 (10.0; 0.8)	41.0 (234.0; 16.0)	20.0 (22.3; 0.9)	17.0 (206.4; 48.9)
2005	30.1 (83.2; 3.5)	17.6 (46.3; 8.5)	23.5 (20.9; 1.7)	27.5 (120.4; 8.3)	16.0 (22.3; 0.9)	20.3 (198.3; 47.0)
2006	24.1 (10.8; 0.5)	46.9 (65.6; 12.0)	12.4 (10.4; 0.8)	30.9 (167.9; 11.5)	19.8 (8.9; 0.4)	37.0 (344.9; 81.7)
2007	21.2 (21.8; 0.9)	11.8 (25.5; 4.7)	– (7.1; 0.6)	47.3 (218.6; 15.0)	25.5 (63.6; 2.6)	14.1 (277.1; 65.6)
2008	41.1 (54.7; 2.3)	17.5 (19.1; 3.5)	31.6 (48.2; 3.8)	37.4 (156.3; 10.7)	15.4 (12.0; 0.5)	31.4 (320.7; 76.0)
2009	18.4 (74.9; 3.2)	27.8 (26.0; 4.8)	– (7.4; 0.6)	27.6 (129.9; 8.9)	28.1 (46.8; 1.9)	11.0 (68.5; 16.2)
2010	45.6 (145.3; 6.1)	29.7 (109.2; 20.0)	23.5 (43.2; 3.4)	21.2 (116.2; 8.0)	– (4.2; 0.2)	10.2 (118.1; 28.0)
2011	40.8 (106.3; 4.5)	45.4 (51.8; 9.5)	– (4.7; 0.4)	55.1 (267.7; 18.4)	43.8 (47.6; 1.9)	10.2 (292.2; 69.2)
2012	28.0 (55.5; 2.3)	16.2 (11.6; 2.1)	16.1 (18.8; 1.5)	58.7 (371.5; 25.5)	24.6 (1.5; 0.1)	58.6 (353.8; 83.8)
2013	25.5 (31.8; 1.3)	26.3 (27.3; 5.0)	20.2 (16.1; 1.3)	60.5 (246.8; 16.9)	14.1 (5.3; 0.2)	16.8 (121.6; 28.8)
2014	32.6 (55.1; 2.3)	26.4 (29.2; 5.3)	18.8 (53.6; 4.3)	56.5 (169.1; 11.6)	47.2 (102.4; 4.1)	10.9 (170.2; 40.3)
2015	49.0 (54.5; 2.3)	14.6 (69.9; 12.8)	– (5.5; 0.4)	46.4 (289.6; 19.9)	40.3 (13.4; 0.5)	13.9 (205.3; 48.6)
2016	41.9 (10.3; 0.4)	34.8 (63.4; 11.6)	14.5 (8.1; 0.6)	59.6 (387.6; 26.6)	37.9 (56.3; 2.3)	23.0 (177.0; 41.9)
B	**33.0 (53.6; 2.3)**	**26.6 (49.8; 9.1)**	**20.4 (15.3; 1.2)**	**44.2 (214.6; 14.7)**	**31.2 (69.3; 2.8)**	**22.0 (179.7; 42.6)**
C	**49.0 (145.3; 6.1)**	**46.9 (109.2; 20.0)**	**31.6 (53.6; 4.3)**	**62.5 (387.6; 26.6)**	**62.3 (247.3; 10.0)**	**58.6 (353.8; 83.8)**

Note. **A**: $[(\Delta pCO_2)_w/(pCO_2)_{wb}]\cdot 100$ % maximum values as determined within *E. huxleyi* blooms in the target seas for each year of satellite observations. **B** and **C**: mean and maximum values of the above ratio over the period of observations. * The number in parenthesis is the area (in 10^3 km^2) of each sea. ** The first and second numbers in parenthesis in each column are, respectively, the maximum bloom area (10^3 km^2) and its ratio to the sea area (in percent).

published reports on ΔpCO_2 in surface water due to *E. huxleyi* blooming in the Black Sea. However, we found that our results obtained on the CO_2 partial pressure within the bloom in the Black Sea proved to be closely in line with the set of multiyear in situ measurements of this variable within an *E. huxleyi* bloom persistently appearing at one and the same station in the area of typical but not most intense blooms of *E. huxleyi* in the Black Sea (south-east off the Crimea) during late May-July in 2009, 2010 and 2013 [Khoruzhiy et al., 2010; Konovalov et al., 2014]. Indeed, the in situ measurements have shown that pCO_2 values were well within the ranges reported by us. Thus, in 2013 pCO_2 levels in the surface waters varied within 420–530 µatm. Through a comparison of these data with those in our Table and assumption that ΔpCO_2 averaged over both the sea and the period of bloom observations in 2015–2016 is 100–120 µatm (Fig. 1, *b*) it can be drawn that our data on pCO_2 are within the range 405–554 µatm. Noting that these numbers refer to the entire bloom area in the Black Sea, the correspondence is close enough and therefore justifies the application of our ΔpCO_2 retrieval algorithm to the Black Sea case.

Thus, the blooming-driven enhancement of atmospheric CO_2 partial pressure over the Black Sea is shown to be caused by the increase in CO_2 partial pressure in water, $(\Delta pCO_2)_w$, whose maximum was in the range 125–150 µatm (Fig. 1, *b*). This corresponds to 44.7–65.8 % of the bloom-driven increase in CO_2 partial pressure in water, assessed as $(\Delta pCO_2)_w$ normalized to CO_2 partial pressure in water in the absence of blooming $(pCO_2)_{wb}$.

Discussion

Importantly, these results for both $(\Delta pCO_2)_w$ and normalized ratio $(\Delta pCO_2)_w/(pCO_2)_{wb}$ are quite comparable with the respective values registered in blooming surface waters of the polar Barents Sea, as well as in some subpolar marine environments, such as the North, Norwegian, Greenland and Bering Seas [Kondrik et al., 2018] – see Table and Figure 4. Hence, a similar blooming-driven

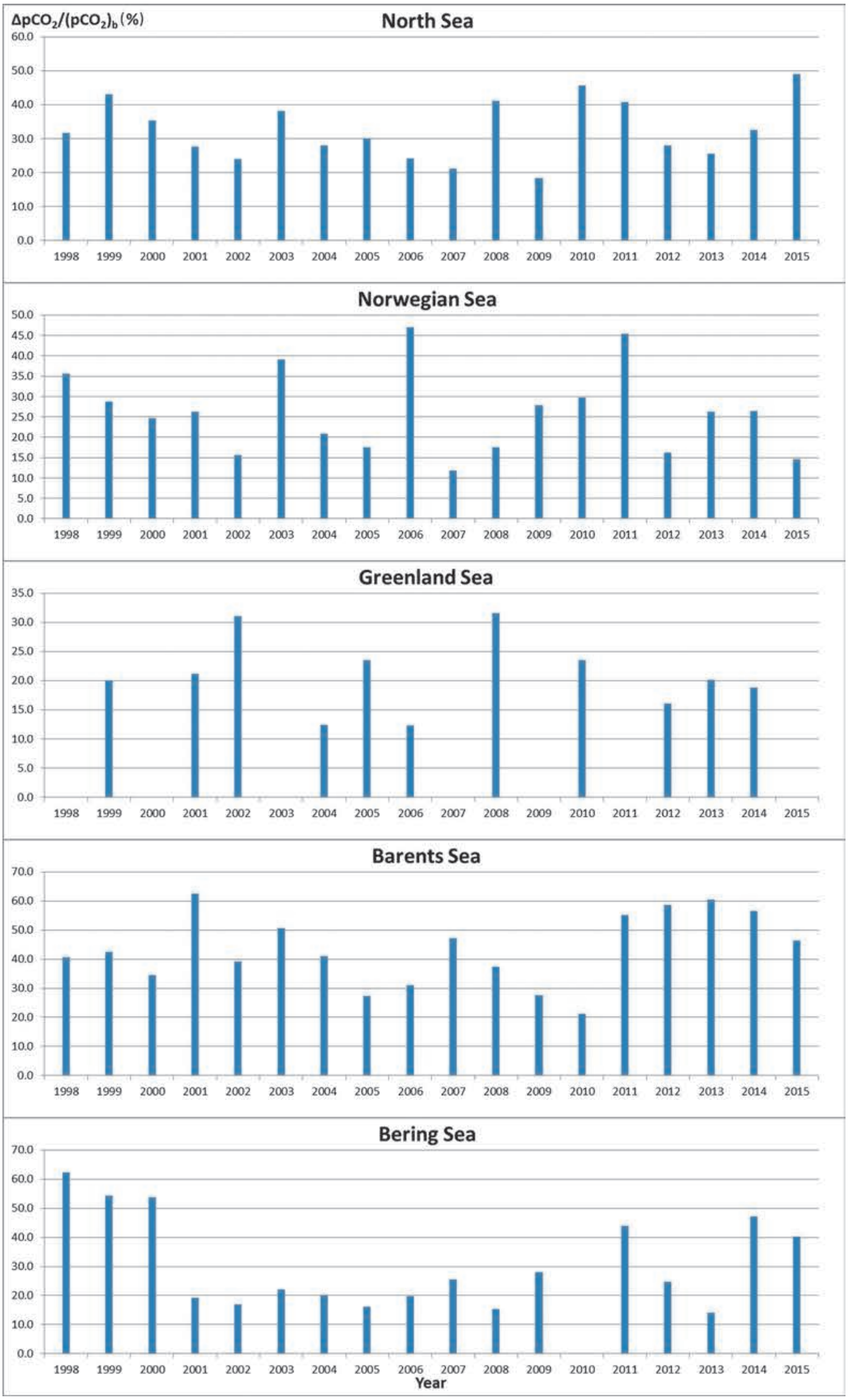

Fig. 4. Spatial and temporal variations in $[(\Delta pCO_2)_w/(pCO_2)_{wb}]\cdot 100$ % maximum values within *E. huxleyi* bloom areas in the North, Norwegian, Greenland, Barents, and Bering Seas during 1998–2015 (Source: [Kondrik et al., 2018]).

The data are absent for some years and target seas as the respective $(\Delta pCO_2)_w$ values proved to be lower than the assessed retrieval error of 23.4 µatm. Some of the y-axes have different scales enhancement of atmospheric CO_2 partial pressure could be expected over them as well. Unfortunately, OCO-2 data on XCO_2 for high latitudes are scarce and generally heavily quality flagged. At least for the two selected years, this precluded a direct determination of ΔXCO_2 over *E. huxleyi* blooms in the subpolar and polar seas mentioned above.

However, since it is the normalized ratio $(\Delta pCO_2)_w/(pCO_2)_{wb}$ that controls the direction of the CO_2 flux in the atmosphere – ocean surface system, the closeness of the normalized ratio values found for such geographically disparate marine environments suggests that the effect of *E. huxleyi* blooms on CO_2 partial pressure increment in marine surface waters is not latitude-longitude specific.

It is also worth of noting that the blooms in the aforementioned seas are not extraordinarily extensive or denser than those in other marine environments in the world's oceans: there are reports on either comparable or even more vast and dense *E. huxleyi* blooms in both Northern and Southern Hemispheres [Brown, Yoder, 1994; Morozov et al., 2013; Balch et al., 2016].

Despite the obvious oneness of the *E. huxleyi* blooming phenomenon at subpolar and polar seas on the one hand and in the Black Sea on the other, one specific feature inherent in the Black Sea is worth mentioning, viz. the moment of the bloom onset: in the Black Sea it occurs much earlier. The registered *E. huxleyi* blooms in the Black Sea in 2015 and 2016 occurred during the time period between late April and late June, with the maximum in mid-May, which is supported by previous observations by e. g. [Oguz & Merico, 2006] see also refs. therein. This specific feature of the *E. huxleyi* outburst timing is known to be controlled by the timing of the preceding photosynthetic phytoplankton mass development. The latter increases the nitrogen to phosphorus (N : P) ratio and creates conditions favoring a successive development of *E. huxleyi* [Tyrrell, Merico, 2004]. Thus, this mechanism of water chemical "preparation" largely (but not exclusively) predetermines the timing of *E. huxleyi* bloom onset. As the outburst and eventual dying off of yearly spring phytoplankton (which are prevalently diatoms) occur in the Black Sea earlier that at high latitudes [Vinogradov et al., 1999; Moncheva et al., 2001], *E. huxleyi* blooms also start developing earlier.

In conclusion, we believe that the results reported here are of relevance to the phenomenon of *E. huxleyi* blooms in general and can be considered as a reference point in future large-scale studies, which are needed in order to attain quantitative assessments of the overall role of *E. huxleyi* blooms in the global carbon cycle.

We express our gratitude for the financial support of this study provided by the Russian Science Foundation (RSF) under the project number 17-17-01117. We also acknowledge the use of the Ocean Colour Climate Change Initiative dataset, Version 3.1, European Space Agency, available online at http://www.esaoceancolour-cci.org/. XCO_2 data were produced by the OCO-2 project at the Jet Propulsion Laboratory, California Institute of Technology, and obtained from the OCO-2 data archive maintained at the NASA Goddard Earth Science Data and Information Services Center.

References

Balch W. M., Bates N. R., Lam P. J., Twining B. S., Rosengard S. Z., Bowler B. C., and Drapeau D. T. Factors regulating the Great Calcite Belt in the Southern Ocean, and its biogeochemical significance. *Global Biogeochem. Cy*. 2016. Vol. 30, no. 8. P. 1124–1144. doi: 10.1002/2016GB005414

Brown C. W., Yoder J. A. Coccolithophorid blooms in the Global Ocean. *J. Geophys. Res.* 1994. Vol. 99. P. 7467–7482. doi: 10.1029/93JC02156

Cokacar T., Kubilay N., and Oguz T. Structure of *Emiliania huxleyi* blooms in the Black Sea surface waters as detected by SeaWiFS imagery. *Geophys. Res. Lett*. 2001. Vol. 28, no. 24. P. 4607–4610. doi: 10.1029/2001GL013770

Crisp D. Measuring atmospheric carbon dioxide from space with the Orbiting Carbon Observatory-2 (OCO-2). *Proceed. SPIE*. Earth Observing Systems XX, 960702 (Sept. 8, 2015). 2015. Vol. 9607. doi: 10.1117/12.2187291

Dlugokencky E. Annual mean carbon dioxide data. NOAA ESRL. 2016.

Garcia H. E., Locarnini R. A., Boyer T. P., Antonov J. I., Baranova O. K., Zweng M. M., Reagan J. R., and Johnson D. R. World Ocean Atlas 2013. Vol. 4: Dissolved inorganic nutrients (phosphate, nitrate, silicate). Eds. S. Levitus, A. Mishonov, Technical Eds. NOAA Atlas NESDIS 76. 2013.

Iglesias-Rodrigues M. D., Brown C. W., Doney S. C., Kleypas J., Kolber D., Kolber Z., Hayes P. K., and Falkowski P. G. Representing key phytoplankton functional groups in ocean carbon cycle models: Coccolithophorids. *Global Biogeochem. Cy*. 2002. Vol. 16, no. 4. P. 47-1-47-20. doi: 10.1029/2001GB001454

IPCC. Climate Change 2014: Synthesis report. Contribution of working groups I, II and III to the Fifth Assessment Report of the Intergovernmental Panel on Climate Change. Eds. Core Writing Team, R. K. Pachauri, L. A. Meyer. IPCC, Geneva, Switzerland, 2014. 151 p.

Key R. M., Olsen A., van Heuven S., Lauvset S. K., Velo A., Lin X., Schirnick C., Kozyr A., Tanhua T., Hoppema M., Jutterström S., Steinfeldt R., Jeansson E., Ishii M., Perez F. F., and Suzuki T. Global Ocean Data Analysis Project, Version 2 (GLODAP v2). 2015. URL: http://cdiac.ornl.gov/oceans/GLODAPv2/ (accessed: 20.06.2019). doi: 10.3334/CDIAC/OTG. NDP093_GLODAPv2

Khoruzhjy D. S., Kondratyev S. I., Medvedev E. V., and Shutov S. A. Dinamika partsial'nogo davleniya uglekislogo gaza i kontsentratsii rastvorennogo kisloroda v shel'fovykh vodakh yuzhnogo berega Kryma v 2009–2010 gg. [Dynamics of the carbon dioxide partial pressure in the Southern Crimea shelf zone in 2009–2010]. *Ekol. bezopasnost' pribrezhnoi i shel'fovoi zon i kompleksnoe ispol'zovanie resursov shel'fa* [J. Ecol. Safety of the Coastal and Shelf Zones and Comprehensive Exploitation of the Shelf Res.]. 2010. Vol. 21. P. 136–145.

Kondrik D., Kazakov E., and Pozdnyakov D. A Synthetic satellite dataset of the spatio-temporal distributions of *Emiliania huxleyi* blooms and their impact on Arctic and Sub-Arctic marine environments (1998–2016). *Earth System Sci. Data*. 2019. Vol. 11. P. 119–128. doi: 10.5194/essd-11-119-2019

Kondrik D. V., Pozdnyakov D. V., and Johannessen O. M. Satellite evidence that *E. huxleyi* phytoplankton blooms weaken marine carbon sinks. *Geophys. Res. Lett.* 2018. Vol. 45, no. 2. P. 846–854. doi: 10.1002/2017GL076240

Kondrik D. V., Pozdnyakov D. V., and Pettersson L. H. Particulate inorganic carbon production within *E. huxleyi* blooms in subpolar and polar seas: A satellite time series study (1998–2013). *Int. J. Rem. Sens*. 2017. Vol. 38, no. 22. P. 6179–6205. doi: 10.1080/01431161.2017.1350304

Konovalov S. K., Kondratyev S. I., Khoruzhiy D. S., Medvedev E. V., and Moiseenko O. G. Obshchii neorganicheskii uglerod, karbonatnaya sistema i potoki uglekislogo gaza v pribrezhnoi zone yuzhnogo berega Kryma: monitoring, kharakteristika, dinamika [Total inorganic carbon, carbonate system and fluxes of carbon dioxide in the Crimean shelf zone: monitoring, characterization, dynamics]. *Monitoring pribrezhnoi zony na Chernomorskom eksperimental'nom podsputnikovom poligone* [Monitoring of the coastal zone in the Black Sea experimental sub-satellite testing area]. Eds. V. A. Ivanov, V. A. Dulov. Sevastopol: NAS of Ukraine, Marine Hydrophysical Institute, 2014. P. 335–372.

Moncheva S., Gotsis O., Pagou K., and Krastev A. Phytoplankton blooms in the Black Sea and Mediterranean coastal ecosystems subjected to anthropogenic eutrophication: similarities and differences. *Estuarine, Coastal and Shelf Sci*. 2001. Vol. 53, no. 3. P. 281–295. doi: 10.1006/ecss.2001.0767

Moore T., Dowel M. D., and Franz B. A. Detection of coccolithophore blooms in ocean color imagery: A generalized approach for use with multiple sensors. *Rem. Sens. Environ.* 2012. Vol. 117. P. 249–263. doi: 10.1016/j.rse.2011.10.001

Morozov E., Pozdnyakov D., Smyth T., Sychev V., and Grassl H. Space-borne study of seasonal, multi-year, and decadal phytoplankton dynamics in the Bay of Biscay. *Int. J. Rem. Sens*. 2013. Vol. 34, no. 4. P. 1297–1331. doi: 10.1080/01431161.2012.718462

Oguz T., and Merico A. Factors controlling the summer *Emiliania huxleyi* bloom in the Black Sea: A modeling study. *J. Marine Syst.* 2006. Vol. 59, no. 3–4. P. 173–188. doi: 10.1016/j.jmarsys.2005.08.002

Olsen A., Key R. M., van Heuven S., Lauvset S. K., Velo A., Lin X., Schirnick C., Kozyr A., Tanhua T., Hoppema M., Jutterström S., Steinfeldt R., Jeansson E., Ishii M., Pérez F. F., and Suzuki T. The Global Ocean Data Analysis Project Version 2 (GLODAPv2) – an internally consistent data product for the World Ocean. *Earth System Sci. Data*. 2016. Vol. 8, no. 2. P. 297–323. doi: 10.5194/essd-8-297-2016

Özsoy E., and Ünlüata Ü. Oceanography of the Black Sea: A review of some recent results. *Earth-Sci. Rev.* 1997. Vol. 42, no. 4. P. 231–272. doi: 10.1016/S0012-8252(97)81859-4

Robertson J. E., Robinson C., Turner D. R., Holligan P., Watson A. J., Boyd P., Fernandez E., and Finch M. The impact of a coccolithophore bloom on oceanic carbon uptake in the northeast Atlantic during summer 1991. *Deep Sea Res.* 1994. Vol. 41, no. 2. P. 297–314. doi: 10.1016/0967

Shutler J. D., Land P. E., Brown C. W., Findlay H. S., Donlon C. J., Medland M., Snooke R., and Blackford J. C. Coccolithophore surface distributions in the North Atlantic and their modulation of the air-sea flux of CO2 from 10 years of satellite earth observation data. *Biogeosciences*. 2013. Vol. 10. P. 2699–2709. doi: 10.5194/bg-10-2699-2013

Smyth T. J., Tyrrell T., and Tarrant B. Time series of coccolithophore activity in the Barents Sea from twenty years of satellite imagery. *Geophys. Res. Lett*. 2004. Vol. 31. doi: 10.1029/2004GL019735

Tyrrell T., and Merico A. Emiliania huxleyi: bloom observations and the conditions that induce them. In *Coccolithophores: from molecular processes to global impact*. Eds. H. R. Thierstein and J. R. Young. Berlin: Springer, 2004. P. 75–97. doi: 10.1007/978-3-662-06278-4_4

Vinogradov M. E., Shushkina E. A., Mikaelyan A. S., and Nezlin N. P. Temporal (seasonal and interannual) changes of ecosystem of the open waters of the Black Sea. In *Environmental Degradation of the Black Sea: Challenges and Remedies*. Eds. S. T. Beşiktepe, Ü. Ünlüata, and A. S. Bologa. NATO Science Partnership Sub-series: 2(56). Dordrecht: Springer Netherlands, 1999. P. 109–129. doi: 10.1007/978-94-011-4568-8_8

Wu L., Hasekamp O., Hu H., Landgraf J., Butz A., aan de Brugh J., Aben I., Pollard D. F., Griffith D. W. T., Feist D. G., Koshelev D., Hase F., Toon G. C., Ohyama H., Morino I., Notholt J., Shiomi K., Iraci L., Schneider M., de Mazière M., Sussmann R., Kivi R., Warneke T., Goo T.-Y., and Té Y. Carbon dioxide retrieval from OCO-2 satellite observations using the RemoTeC algorithm and validation with TCCON measurements. *Atmos. Meas. Tech*. 2018. Vol. 11. P. 3111–3130. doi: 10.5194/amt-11-3111-2018

Received July 08, 2019

СВЕДЕНИЯ ОБ АВТОРАХ:

Кондрик Дмитрий Вячеславович
научный сотрудник
Научный фонд «Международный центр по окружающей среде и дистанционному зондированию имени Нансена»
14-я линия В. О., оф. 49, Санкт-Петербург, Россия, 199034
эл. почта: dmitry.kondrik@niersc.spb.ru

Казаков Эдуард Эдуардович
научный сотрудник
Научный фонд «Международный центр по окружающей среде и дистанционному зондированию имени Нансена»
14-я линия В. О., оф. 49, Санкт-Петербург, Россия, 199034
эл. почта: ekazakov@niersc.spb.ru

Поздняков Дмитрий Викторович
заместитель директора по науке, руководитель группы водных экосистем, д. ф.-м. н., проф.
Научный фонд «Международный центр по окружающей среде и дистанционному зондированию имени Нансена»
14-я линия В. О., оф. 49, Санкт-Петербург, Россия, 199034
эл. почта: dmitry.pozdnyakov@niersc.spb.ru

Йоханнессен Ола Матиас
Президент Научного Общества имени Нансена;
Президент Уставного Фонда Нансен-Центров в Норвегии и Санкт-Петербурге; Почетный профессор Геофизического Института при университете Бергена, Норвегия
Берген, Норвегия, 5006
эл. почта: ola.johannessen@nansenscientificsociety.no

CONTRIBUTORS:

Kondrik, Dmitry
Scientific Foundation “Nansen Environmental and Remote Sensing Centre”
14th Line, 7, Office 49, Vasilievsky Island, 199034
St. Petersburg, Russia
e-mail: dmitry.kondrik@niersc.spb.ru

Kazakov, Eduard
Scientific Foundation “Nansen Environmental and Remote Sensing Centre”
14th Line, 7, Office 49, Vasilievsky Island, 199034
St. Petersburg, Russia
e-mail: ekazakov@niersc.spb.ru

Pozdnyakov, Dmitry
Scientific Foundation “Nansen Environmental and Remote Sensing Centre”
14th Line, 7, Office 49, Vasilievsky Island, 199034
St. Petersburg, Russia
e-mail: dmitry.pozdnyakov@niersc.spb.ru

Johannessen, Ola
Nansen Scientific Society; Nansen Centres in St. Petersburg and Bergen; Geophysical Institute, University of Bergen
Kong Christian Frederiks Plass 6, 5006 Bergen, Norway
e-mail: ola.johannessen@nansenscientificsociety.no